Terr. Atmos. Ocean. Sci., Vol. 24, No. 3, 323-332, June 2013 doi: 10.3319/TAO.2012.11.26.01(TT)

Spatial Variations of Soil Gas Geochemistry in the Tangshan Area of Northern China

Ying Li[1, *], Jianguo Du[1], Xin Wang[2], Xiaocheng Zhou[1], Chao Xie[1], and Yueju Cui[1]

[1] *CEA Key Laboratory of Earthquake Prediction, Institute of Earthquake Science, China Earthquake Administration, Beijing, China*
[2] *Earthquake Administration of Shanxi Province, Xi'an, China*

Received 30 November 2011, accepted 26 November 2012

ABSTRACT

The concentrations of Hg, Rn, H_2, He and CO_2 in soil gases at 756 sites were measured in the Tangshan area where M_s 7.8 earthquake occurred in 1976 and is characterized by complex tectonic structures and high seismic hazard. The results showed that, spatial variations of the gaseous anomalies, especially hydrogen and helium have spatial congruence along the tectonic lines, which can be attributed to their deep sources and the migration paths formed by the faults. A better congruence of radon and carbon dioxide is highlighted which indicates that carbon dioxide acts as the carrier gas for radon in this area. Two geochemical anomaly zones of soil gas were found in the area wherein all the studied gases exhibited anomalies or high values, related to the faults and earthquakes.

Key words: Soil gas, Geochemistry, Fault activity, The Tangshan area

Citation: Li, Y., J. Du, X. Wang, X. Zhou, C. Xie, and Y. Cui, 2013: Spatial variations of soil gas geochemistry in the Tangshan area of Northern China. Terr. Atmos. Ocean. Sci., 24, 323-332, doi: 10.3319/TAO.2012.11.26.01(TT)

1. INTRODUTION

The geochemical characteristics and behavior of soil gases (Rn, Hg, He H_2 and CO_2) in seismically active areas have been investigated widely for correlating geochemical variations with faults and earthquake activities (Ciotoli et al. 1999, 2007; Du et al. 2008; Wiersberg and Erzinger 2008; Woodruff et al. 2009; Lombardi and Voltattorni 2010). Some gas-geochemical precursors for the earthquakes were determined and have been applied for active fault identification (Walia et al. 2010) and earthquake study (Evision 2001; Walia et al. 2006; Yang et al. 2006). The fluids with different chemical compositions filled in faults and fractures in the crust can be activated and migrate up to the surface under the pressure and temperature changes related to crust deformations and earthquakes (Bernard 2001). Therefore, there exists a good correlation between the concentration of soil gases and the stress/strain in the crust (Yang et al. 2006; Utkin and Yurkov 2010). Consequently, soil gases are often used as good tracers for fault activity and earthquake.

Gas discharge through seismically active faults is a long and permanent process. Active faults can be a function as 'drains' in the crust which sustains the gas geochemical characteristics of a certain area. Therefore, the determination of soil gas geochemical characteristics in an active fault area must be based upon the background values and spatial distribution (Gupta 2001; Wiersberg and Erzinger 2008; Li et al. 2009). The fluxes of soil gases are controlled by many factors in different ways including mantle degassing, tectonic geometry, atmospheric permutation, biogenic process, radiogenic production, and rock alteration. (Hinkle 1994; Ciotoli et al. 2007) which indicates that the gaseous species in soil have multiple sources and their concentrations are due to different factors. Thus, it has been emphasized that increasing the density of monitoring sites (high-density sampling sites) and components (multiple indicators) can be a better solution for well understanding the soil gas geochemical background and earthquake precursors in a seismic area (Ciotoli et al. 2007; Walia et al. 2010).

The goal of this paper is to correlate geochemical variations of soil gases and active faults in the Tangshan Area of North China and discuss the coupling usefulness between

* *Corresponding author*
E-mail: subduction6@hotmail.com

different soil gas components and fault delineations based on the data of soil gases measured in the field. Our results are helpful for the sites selection of continuous geochemical monitoring aiming at earthquake precursor capture and regional seismic activity detection in the study area.

2. SEISMOGEOLOGICAL SETTINGS

The Tangshan area is located in a fold-depression region where the Northern China plain and the Yanshan uplift are converged. Surrounded by four active faults (F1, F2, F3, and F4, Fig. 1), the Tangshan area can be spatially characterized as a 'rhombic block.' The basement of the Tangshan area is composed of Pre-Sinian metamorphic rocks with varying metamorphic grades whose outcrops rarely occur in the study area covered by the thick sediments of the Holocene (Q_4) and upper Pleistocene (Q_3) (Fig. 1). The studies of seismic exploration, gravimetric and electrical surveys (Mei et al. 1982) in the area indicated the following characteristics of the active faults (Fig. 1):

F1: the Fengtai-Yejituo Fault with NEE trending NW dipping in the western segment but SE dipping in the northeastern segment is located at the northwestern edge of the rhombic block.

F2: the Jiyunhe Fault in the southwestern sector formed in the early Paleozoic Era and reactivated until the Caenozoic Era is generally with SW dipping and NW trending in the northwest part, but gently westward trending in the southeastern part, which is the seismogenic fault of the 1976 Ninghe M_s 6.9 earthquake.

F3: the Ninghe-Changli Fault with NE trending and SE dipping at the south edge of the rhombic block, was formed in the early Sinian Period and has reactivated

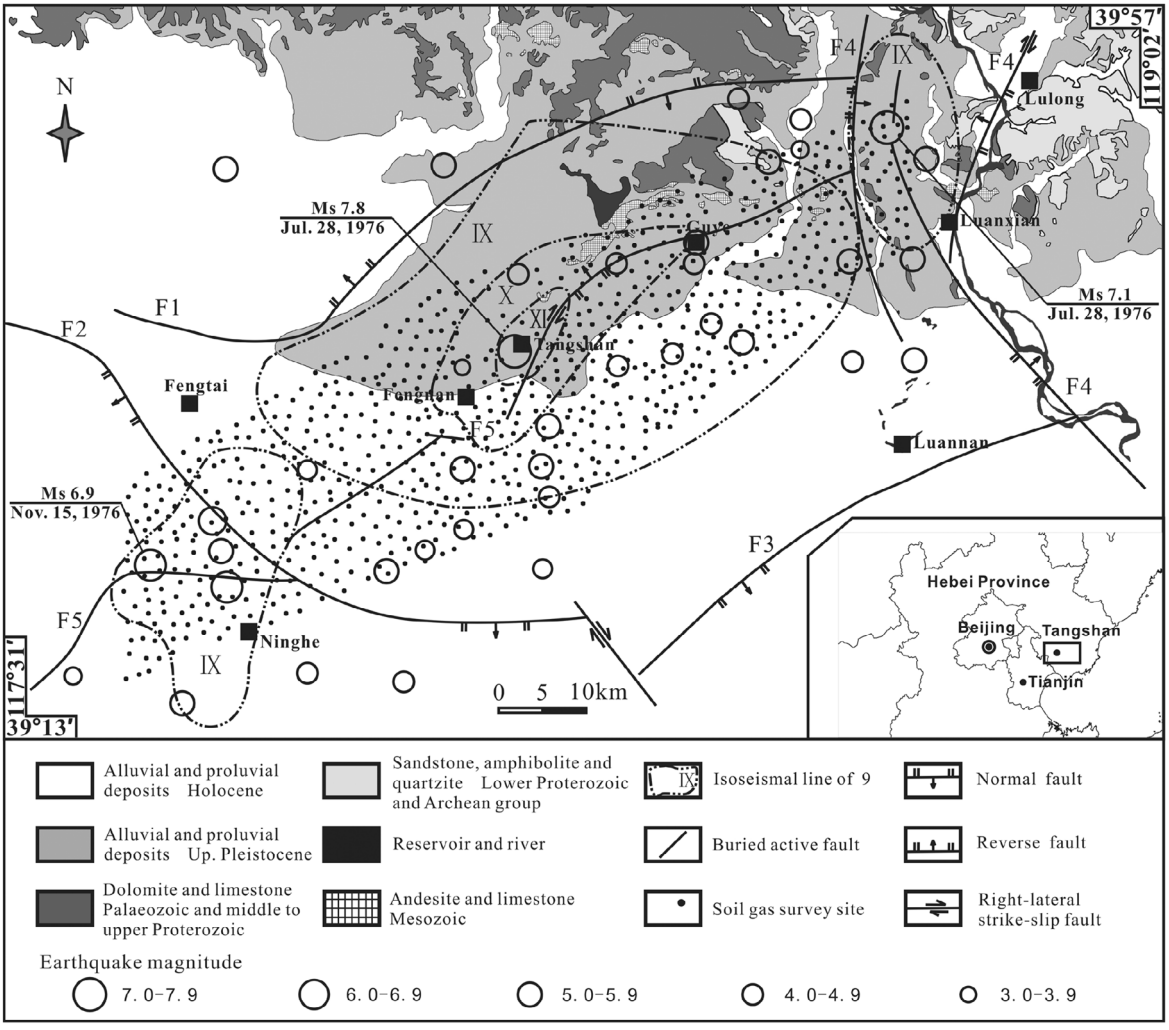

Fig. 1. Simplified geological map of the Tangshan area, Northern China (modified after Mei et al. 1982; Chen et al. 1998) with the sampling sites for soil-gas analysis and the epicenters (the earthquakes recorded with intact information are available since 1624 to 2010, data from China Earthquake Networks Center). The epicenters of $M_s \geq 3.0$ since 1624 mainly distribute along F5 in the study area selected here. F1: Fengtai-Yejituo fault, F2: Jiyunhe fault, F3: Ninghe-Changli fault, F4: Luanxian- Laoting fault, F5: Tangshan fault.

intensively since the Mesozoic Era, especially by the 1976 Tangshan M_s 7.8 earthquake.

F4: the Luanxian-Laoting Fault as the eastern boundary of the rhombic block can be divided into four segments, three are with NW-NNE trending and NE dipping in the west part and one with NE trending and NW dipping in the east part. The fault formed in the early Paleozoic Era reactivated intensively in the Cenozoic Era, and was designated as the seismogenic fault of the 1976 Luanxian M_s 7.1 earthquake.

F5: the Tangshan Fault across the center of the rhombic block, composed of several segments, is a normal fault with a right lateral strike slip and has a NE trending and NW dipping with a high dip angle which reactivated during the Ninghe M_s 6.9 and Luanxian M_s 7.1 earthquakes in 1976. The Tangshan fault was considered to be a strain-accumulation structure interacted with F2 and F4 in the 'rhombic block' (Nábělek et al. 1987). The 1976 Tangshan main shock was interpreted as a complex tectonic process of strike-slip, thrust and normal-fault events along the Tangshan fault (Butler et al. 1979) caused by the detachment, fault-propagation in the middle crust and the stress accumulation in the base of upper crust.

Geology, seismic exploration and electrical survey results showed that the active faults (F1 - F5) dislocated the strata of the Cenozoic Era (Mei et al. 1982). The thickness of Q_4 and Q_3 increases from about 100 m in the north to 800 m in the south was controlled by the activation of F3 in the rhombic block. Archeology results showed that the position of ancient shoreline moved about 40 km from north to south since the Neolith in the area. Consequently, the Tangshan rhombic block has been highly active since the Cenozoic Era companied frequently with the seismic events. The latest large event occurred in 1976 in Tangshan caused more than 240000 death toll and extended the seismic intensity zones along the Tangshan Fault. The epicenters with intact information which have been recorded in the area since 1624 are mainly distributed along the Tangshan Fault (Fig. 1).

3. SOIL GAS SURVEY

A target area of about 2500 km^2 (Fig. 1) was delineated carefully and covered the earthquake epicenters and the active faults (F5, F2 and F4). The concentrations of Hg, Rn, CO_2, H_2 and He in soil gas at 756 sampling sites were measured in the field at approximately 1.5-km interval between each two sampling sites. The emission of deep-source gases can be affected by soil moisture, air temperature and barometric pressure (Hinkle 1994); thus from 8th April to 7th May, spring, 2010, a period of stable meteorological conditions in North China was selected for the soil gas survey in this work. The Tangshan area is located along North latitude 39° - 40° (Fig. 1) with a warm temperate semi-humid continental monsoon climate. The air temperature (7.1 - 19.6°C in average), wind velocity (3 - 5 m s^{-1} in average) and direction (south) remains relatively stable and rainfall (21.3 mm) is less in spring than the mean annual rainfall (610 mm) in the area (www.weather.com.cn). Furthermore, in order to minimize the effect of climate on the measuring result, all the sampling and measuring process were conducted in the field from 9:30 am to 17:30 pm.

3.1 Sampling Procedure

The sampling and analytical protocols followed the method described by Zhou et al. (2007) and Li et al. (2009). At a sampling site, three holes of 1 m deep and 3 cm in diameter at 0.5 m lateral intervals were obtained by driving a steel rod into the soil. We used hollow Teflon tube probes with 0.03 m in diameter for gas collection, which were inserted into the holes at about 0.8 m in depth. The Teflon probe was specially designed to be cone-shaped on the top with 0.2 m in length in order to prevent air from entering. The root side was perforated for soil gas collection at the required depth. Using rubber tubes, one probe was connected to a radon detector and the other two were connected to a mercury detector (Fig. 2).

3.2 Instruments and Measuring Process

An HDC-B Radon Detector was employed for the radon concentration measurement. The instrument has a calibration error of less than 5%, calibrated in the standard radon chamber at the Airborne Survey and Remote Sensing Center of Nuclear Industry, China. The instrument operates based on the emission of α-particles during the decay of ^{222}Rn to ^{218}Po and ^{214}Po. An α-sensitive scintillation cell converts radiation to light energy, which is then converted to an electrical impulse by a photomultiplier and recorded by an electronic circuit. The detection limit of the radon detector is 300 Bq m^{-3}. During the measurement, a film sampler was inserted into the sampling chamber for α-particles collection and then air in the sampling chamber (2 L volume) of the instrument was expelled through iterative pumping the soil gas in. When the chamber pressure was pumped up to 1.5×10^5 pa, the sampling process was started. After 3 min sampling, the film sampler was transported into the instrument for radon counting.

The concentration of Hg was attained by a RA-915+ Zeeman Effect atomic absorption spectrometer, which is designed for the direct determination (without the preconcentration in the absorption trap) of mercury concentrations in soil gas (Sholupov et al. 2004). The analyzing data was gained in the gas measuring mode of the instrument. The error of measurements is 2 ng m^{-3}, the detection limit is 1 ng m^{-3}.

CO_2, He and H_2 were analyzed with an Agilent 3000 gas chromatography (GC) instrumented a thermal conductivity detector (TCD) with an error of 5%. To prevent air contamination, soil gases were sampled from the gas circuit of the Radon sampling device with a glass syringe, and injected directly into the GC. The detection limit of CO_2, He and H_2 is 2 ppm.

The measurement procedures above were duplicated at least 2 times at every sampling site to confirm the measuring result.

4. RESULTS AND DATA PROCESSING

4.1 Statistical Analysis and Anomaly Threshold

Using the SPSS 13.0 software package, descriptive and statistic results of the soil gas data are obtained (Table 1). Concentrations of all five soil gases showed spatial variations and were found to be much higher than their concentrations in the atmosphere (Novelli et al. 1999; Ciotoli et al. 2007). The mean and median values highlight that the frequency distribution of the gases are positively skewed by the presence of outliers, indicating abnormal sample distributions. Rn, CO_2, Hg and H_2 have low dispersed distributions relative to He indicated by the skewness values (2.2, 2.0, 1.8, 2.7 and 5.2, respectively). The main statistical parameters including the means and medians values as well as both the SD and IQR values of the soil gas data confirm an abnormal distribution for all variables; even if the data were log transformed, with the exception of Rn, the soil gas values still do not follow a normal distribution (sig. < 0.05 in Kolmogorov-Smirnov test). The Quantile-Quantile plot (Q-Q plot) method has been used to calculate the anomalous values and extra outliers (Sinclair 1991). The method is more objective than the others used to identify the anomaly threshold. The anomaly thresholds are identified as Hg, Rn, H_2, He and CO_2 and are 17.0 ng m^{-3}, 8294.1 Bq m^{-3}, 9.6, 5.3, and 2320.4 ppm, respectively (Fig. 3).

4.2 Contour Line Map Processing

The contour line maps (Fig. 4) were built using the computer-processed 'Kriging' interpolation method in the

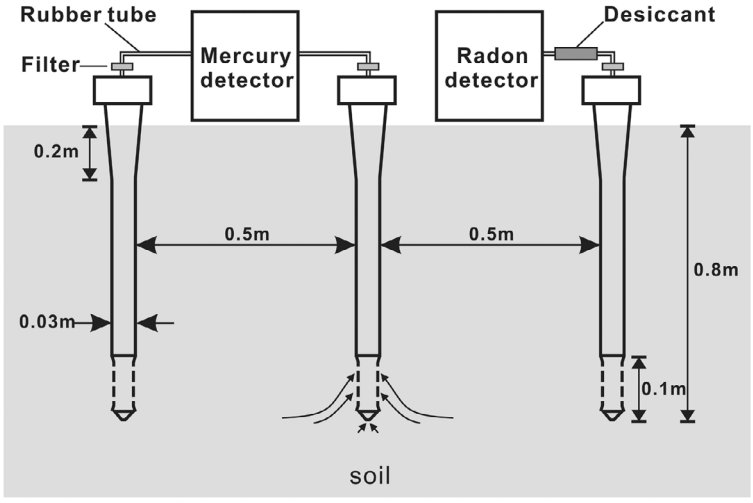

Fig. 2. Sampling scheme employed for soil-gas measurement.

Table 1. Main statistic parameters of soil gas data in the Tangshan area.

	Samples	Mean	Median	Min	Max	Lower Quartile	Upper Quartile	IQR	SD	Skewness	Anomaly threshold
Hg, ng m^{-3}	756	12.0	10.0	2.0	61.0	6.0	15.0	9.0	8.6	1.8	17.0
Rn, Bq m^{-3}	756	5550.4	3882.4	411.8	38470.6	2121.1	7058.8	4937. 7	4992.6	2.2	8294.1
H_2, ppm	756	7.7	4.8	2.0	60.3	3.5	9.9	6.4	7.0	2.7	9.6
He, ppm	756	5.4	4.4	≤ 2.0	47.2	3.6	6.1	2.4	3.0	5.2	5.3
CO_2, ppm	756	2777.6	1734.8	499.0	19760.3	1170.4	3133.2	1962.8	2551.9	2.0	2320.4

Note: The parameters were calculated using the SPSS 13.0 software package. The anomaly threshold was identified by the Quantile-Quantile plots (Fig. 3).

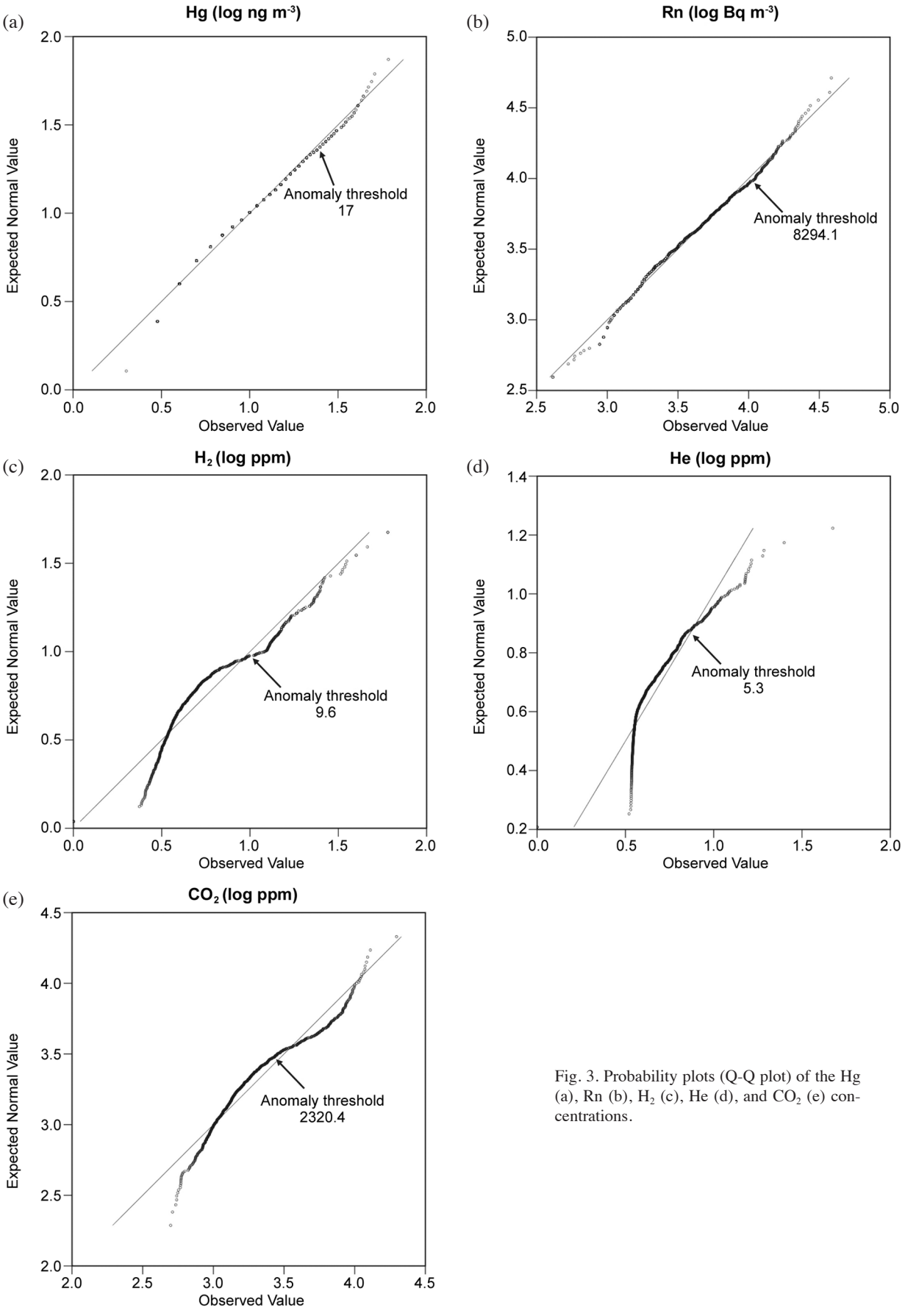

Fig. 3. Probability plots (Q-Q plot) of the Hg (a), Rn (b), H_2 (c), He (d), and CO_2 (e) concentrations.

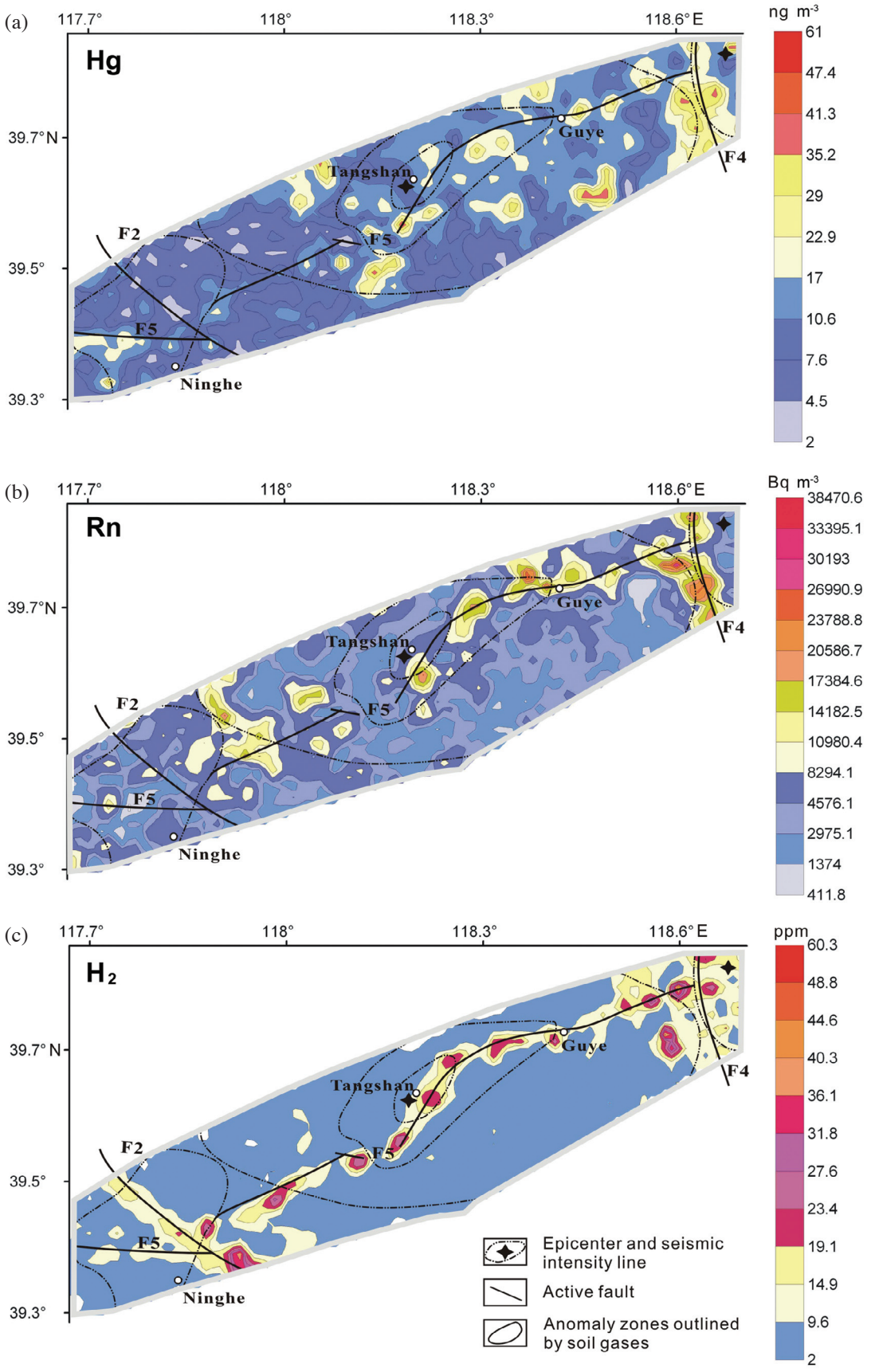

Fig. 4. Contour maps of Hg (a), Rn (b), H_2 (c), He (d), and CO_2 (e) concentrations in the Tangshan area show that the anomalies fit well with the trend of structural features in the survey area. H_2 and He have highly correlative tendency with active faults.

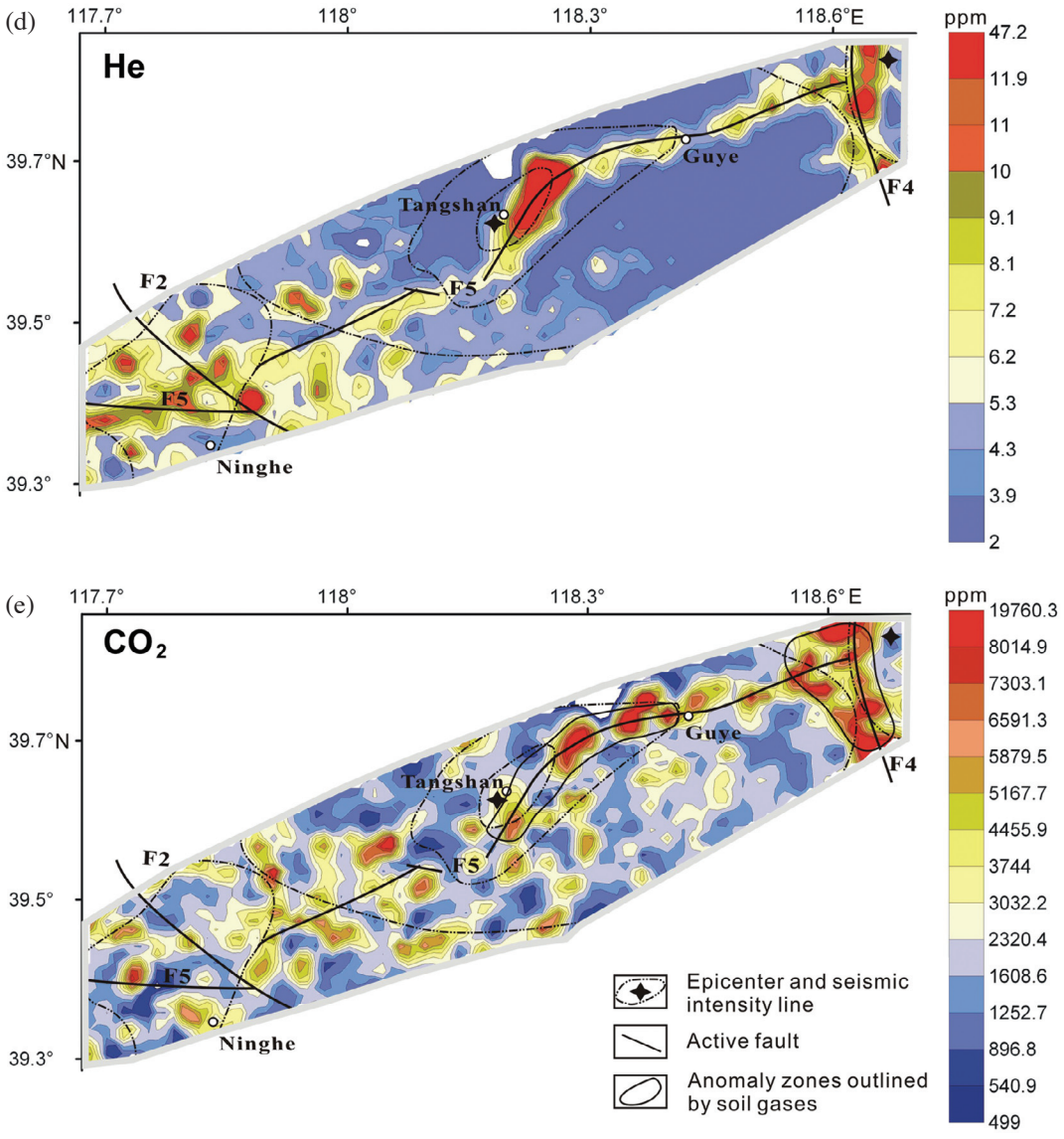

Fig. 4. (Continued)

SURFER 8.0 package (Surface Mapping System, Golden Software, Inc). The color scale of each map was produced considering the anomaly threshold values determined by Q-Q plots. It is well understood that geochemical data are evidently characterized by the variation of concentration values at different sites. The spatial variations are demonstrated by different color gradations. The areas with the soil gas values lower than their thresholds were denoted by blue color, the other areas with higher values were colored from straw yellow to carmine. The contour line maps (Fig. 4) illustrate that the anomalies of H_2 and He were localized mainly along F2, F4 and F5, for Hg, Rn and CO_2 high values were mainly obtained along F4 and the eastern part of F5 indicating that the anomalies of soil gases are dominated by the seismogenic faults.

5. DISCUSSION

5.1 Spatially Characteristics of Soil Gas Concentrations and Interpretation

Our results show that the anomalous patterns of soil gases in the Tangshan area mainly appeared in belt zones along the active faults. Especially H_2 and He have higher correlative trends with tectonic lines. This is attributed to (1) the massive intrusions in the upper and middle crust which derived from the upper mantle. According to a study of 3D S-wave velocity structure using a receiver-function inversion technique and teleseismic P waveform data (Liu et al. 2007), there exist obvious heterogeneous low-velocity materials in the upper and middle crust of the Tangshan area. The crust-mantle boundary has an obvious block-uplift

and the top anomalous boundary of the upper mantle is 10 km beneath the Tangshan block. Consequently, the materials from the deep mantle could be a source origin of the soil gases. (2) The active faults (F2, F4 and F5) with soil gas anomalies detected in the study area have been identified to be deeply penetrating faults and penetrate the crust (Mei et al. 1982) which formed the paths for deep-seated gases migrating up to the ground.

However, for Hg and Rn, anomaly values scarcely appeared along F2 and the western segment of F5; some low values of Hg (< 4.5 ng m^{-3}) and Rn (< 2975.1 Bq m^{-3}) occurred along F2. This should be attributed to the high soil moisture caused by the low ground water level and the wide distribution of water reservoirs in the west part of Tangshan area. Experimental study (Song and Heyst 2005) shows that high initial soil moisture can prevent the emissions of gaseous mercury because of the physical displacement of interstitial soil air containing Hg. The same conclusion also has been obtained by Poissant et al. (2004) based on a continuous field monitoring of mercury gas exchanges in the bay St. Francois wetlands (Québec, Canada). Under wet conditions (flood, river, lakes, swamp et al.), labile mercury from sediments (the one available for air-soil gas exchange) would contribute less to surface gas exchange since it is retained more in the water column.

A positive correlation between emanation coefficient of Rn and soil moisture were determined by the investigation of Washington and Rose 1992. However, this conclusion is only suitable for the unsaturated water cases. If the vapor content in soil increases and reaches saturated conditions, the emanation coefficient of Rn will decrease sharply which has been identified by experiments (Menetrez et al. 1996) and field studies (Wang et al. 2006). This is the reason for less anomalies of Rn observed in the west part of the study area. Evidently, soil moisture is a main factor affecting the geochemical distribution of Hg and Rn in soil in this study.

Conversely, H_2 and He concentrations in soil gases are rarely affected by soil moisture because they are highly insoluble in water, highly mobile and able to pass through thick sediment layer to form anomalies near the ruptures (Andrews 1983). Thus a clearly spatial correlation between the faults and the anomalies of H_2 and He are exhibited in Fig. 4. In the study area, higher concentration values of H_2 (in the range of 19.1 - 60.3 ppm) occurred mainly along F5 (Fig. 4c). Soil H_2 concentrations in the area with more intensive and frequent earthquakes are significantly higher than that from the areas associated with less or no earthquakes (Dogan et al. 2007), which could be attributed to H_2 generated from the chemical reaction between water and tectonically-induced fractures of silicate rocks (Wakita et al. 1980). F5 was associated with the most intensive earthquakes and aftershocks in the area (Fig. 1); more fractures of silicate rocks occurred along it as described above which provided an additional source of H_2 beside the deep source. Consequently, H_2 concentrations along F5 are significantly higher than that near F2 and F4.

For CO_2, some 'spotty anomalies' (isolated points with high values) appeared apart from the faults. The Quaternary sediments (Q_4 and Q_3) in the survey area are on average 400 meters in thickness and no active or ancient volcanic event was historically recorded in the Tangshan area (Mei et al. 1982). Thus, the spotty anomalies of CO_2 can be attributed to organic material oxidation, microorganism or plant respiration and the existence of coal beds beneath the Cenozoic sediments.

5.2 Carrier Gas of Radon

The possible carrier gases of Rn have been identified to be CO_2 or CH_4 with a fast-flowing rate in soil gas (Yang et al. 2003; Fu et al. 2008). Thus, CO_2 always has a good correlation with ^{222}Rn in soil gas; the correlation coefficient between CO_2 and Rn is 0.70 and 0.50 in the eastern and western sector respectively of Fucino Plain, Italy (Ciotoli et al. 2007); 0.49 along Hsinhua fault, southern Taiwan (Walia et al. 2010). In this study, a better congruence of Rn and CO_2 is highlighted by the correlation coefficient of 0.81, although in the counter map (Fig. 4f) some isolated points with high CO_2 values presented. Thus, CO_2 acts as the carrier gas for Rn in the Tangshan area.

5.3 Geochemical Anomaly Zones of Soil Gas

Two geochemical anomaly zones of soil gases can be determined in the Tangshan area according to this study (Fig. 2e). One is the banded zone along the east segment of F5 between Tangshan and Guye; the other is the trapezium zone along F4. All the studied gas species exhibited anomaly values in the anomaly zones. The formation of the anomaly zones could be interpreted as that (1) in the anomaly zones, earthquakes with higher seismic scales occurred. The epicenters of the main shock (M_s 7.8 Tangshan earthquake) and the largest aftershock (M_s 7.1 Luanxian earthquake) were located near the two anomaly zones respectively where the crust has suffered more intensive stress disturbance and breakages. (2) According to the study of the Tangshan aftershock sequence by short-period seismograms (Shedlock et al. 1987), the depths of the aftershocks in the area ranged from 9 to 20 km, deeper than most intraplate earthquake sequences (Meissner and Strehlau 1982). There were 19 aftershocks with $M_l \geq 4.0$ deeper than 18 km and were superimposed on the faults in the present study area. 12 aftershocks were located in the anomaly zones and 7 aftershocks distributed along F2 and the western segments of F5. Thus, the crust in the two zones outlined was shocked by more deeper-aftershocks relative to the other areas. In this case, more fractures and paths were produced by the aftershocks for the migration of the gases from lower mantle/

deep crust up to the ground.

Consequently, the anomaly zones determined are geochemistry-sensitive and suitable for soil gas monitoring of earthquake precursors obtaining and regional seismic activity detection.

6. CONCLUSIONS

The spatial variations of soil gases (Rn, Hg, He, H_2 and CO_2) in the Tangshan area were studied based on the measuring results at 756 sampling sites. The results indicated that the anomalies of the soil gases have an obvious correlation with the fault extending in the area attributed to the deeper fractures and earthquakes.

Due to the soil moisture, Hg and Rn showed fewer anomalies in the west region. CO_2 presented some spotty distributions in the study area caused by the microorganisms, plant respiration, mobility and solubility of the gases. However, a clear spatial correlation between the faults and the anomalies of H_2 and He are exhibited in the entire study area. Thus, it can be concluded that the measurements of more gas species provide more reliable information for geochemical characteristics and fault mapping in a given area. Compared with the other gas species, H_2 and He concentrations are affected less by environmental (soil) factors. This research also confirmed the conclusion of recent studies (Ciotoli et al. 2007; Walia et al. 2010) that CO_2 may act as the main carrier gas for Rn, even its concentration can be easily affected by hyper genesis factors.

Two geochemical anomaly zones of soil gases were outlined in the area, caused by larger earthquakes and the aftershocks with deeper focal depths. The anomaly zones could be suitable sites for continuous monitoring of soil gases aiming at earthquake precursors obtaining and regional seismic activity detection in the Tangshan area.

Acknowledgements We are grateful to the Seismological Bureau of Tangshan city and Dr. Baojun Yin for help in the field survey. This work was financially supported by the Basic Research Project of Institute of Earthquake Science, CEA (02092433; 0212241503). We thank the two anonymous reviewers whose criticisms and suggestions helped to greatly improve the article. We are also grateful to the kind help by the Editor Professor Tsanyao Frank Yang and Mei-Ling Chen.

REFERENCES

Andrews, J. N., 1983: Dissolved radioelements and inert gases in geothermal investigations. *Geothermics*, **12**, 67-82, doi: 10.1016/0375-6505(83)90019-6. [Link]

Bernard, P., 2001: From the search of 'precursors' to the research on 'crustal transients'. *Tectonophysics*, **338**, 225-232, doi: 10.1016/S0040-1951(01)00078-6. [Link]

Butler, R., G. S. Stewart, and H. Kanamori, 1979: The July 27, 1976 Tangshan, China earthquake - A complex sequence of intraplate events. *Bull. Seismol. Soc. Am.*, **69**, 207-220.

Chen, G. X., L. R. Zhang, W. J. Wang, Z. W. Chen, Y. Y. Xu, and K. B. Wei, 1998: Center for Analysis and Prediction, China Seismological Bureau, Earthquake and active fault map of the Capital Region, China, Scale 1:500000.

Ciotoli, G., G. Etiope, M. Guerra, and S. Lombardi, 1999: The detection of concealed faults in the Ofanto Basin using the correlation between soil-gas fracture surveys. *Tectonophysics*, **301**, 321-332, doi: 10.1016/S0040-1951(98)00220-0. [Link]

Ciotoli, G., S. Lombardi, and A. Annunziatellis, 2007: Geostatistical analysis of soil gas data in a high seismic intermontane basin: Fucino Plain, central Italy. *J. Geophys. Res.*, **112**, B05407, doi: 10.1029/2005JB004044. [Link]

Dogan, T., T. Mori, F. Tsunomori, and K. Notsu, 2007: Soil H_2 and CO_2 surveys at several active faults in Japan. *Pure Appl. Geophys.*, **164**, 2449-2463, doi: 10.1007/s00024-007-0277-5. [Link]

Du, J., X. Si, Y. Chen, H. Fu, and C. Jian, 2008: Geochemical anomalies connected with great earthquakes in China. In: Stefánsson, Ó. (Ed.), Geochemistry Research Advances, Nova Science Publishers, Inc., New York, 57-92.

Evison, F. F., 2001: Long-range synoptic earthquake forecasting: An aim for the millennium. *Tectonophysics*, 338, 207-215, doi: 10.1016/S0040-1951(01)00076-2. [Link]

Fu, C. C., T. F. Yang, J. Du, V. Walia, Y. G. Chen, T. K. Liu, and C. H. Chen, 2008: Variations of helium and radon concentrations in soil gases from an active fault zone in southern Taiwan. *Radiat. Meas.*, **43**, S348-S352, doi: 10.1016/j.radmeas.2008.03.035. [Link]

Gupta, H. K., 2001: Short-term earthquake forecasting may be feasible at Koyna, India. *Tectonophysics*, **338**, 353-357, doi: 10.1016/S0040-1951(01)00083-X. [Link]

Hinkle, M. E., 1994: Environmental conditions affecting concentrations of He, CO_2, O_2 and N_2 in soil gases. *Appl. Geochem.*, **9**, 53-63, doi: 10.1016/0883-2927(94)90052-3. [Link]

Li, Y., J. Du, F. Wang, X. Zhou, X. Pan, and R. Wei, 2009: Geochemical characteristics of soil gas in the Yanhuai basin, northern China. *Earthq. Sci.*, **22**, 93-100, doi: 10.1007/s11589-009-0093-3. [Link]

Liu, Q., J. Wang, J. Chen, S. Li, and B. Guo, 2007: Seismogenic tectonic environment of 1976 great Tangshan earthquake: Results given by dense seismic array observation. *Earth Sci. Front.*, **14**, 205-213. (in Chinese)

Lombardi, S. and N. Voltattorni, 2010: Rn, He and CO_2 soil gas geochemistry for the study of active and inactive

faults. *Appl. Geochem.*, **25**, 1206-1220, doi: 10.1016/j.apgeochem.2010.05.006. [Link]

Mei, S. R., C. H. Hu, C. Z. Zhu, J. Ma, Z. C. Zhang, and M. Y. Yang, 1982: The 1976 Tangshan Earthquake, Seismological Press, Beijing. (in Chinese)

Meissner, R. and J. Strehlau, 1982: Limits of stresses in continental crusts and their relation to the depth-frequency distribution of shallow earthquakes. *Tectonics*, **1**, 73-89, doi: 10.1029/TC001i001p00073. [Link]

Menetrez, M. Y., R. B. Mosley, R. Snoddy, and S. A. Brubaker Jr., 1996: Evaluation of radon emanation from soil with varying moisture content in a soil chamber. *Environ. Int.*, **22**, S447-S453.

Náběl ek, J., W. P. Chen, and H. Ye, 1987: The Tangshan earthquake sequence and its implications for the evolution of the North China basin. *J. Geophys. Res.*, **92**, 12615-12628, doi: 10.1029/JB092iB12p12615. [Link]

Novelli, P. C., P. M. Lang, K. A. Masarie, D. F. Hurst, R. Myers, and J. W. Elkins, 1999: Molecular hydrogen in the troposphere: Global distribution and budget. *J. Geophys. Res.*, **104**, 30427-30444, doi: 10.1029/1999JD900788. [Link]

Poissant, L., M. Pilote, P. Constant, C. Beauvais, H. H. Zhang, and X. Xu, 2004: Mercury gas exchanges over selected bare soil and flooded sites in the bay St. FranÇois wetlands (Québec, Canada). *Atmos. Environ.*, **38**, 4205-4214, doi: 10.1016/j.atmosenv.2004.03.068. [Link]

Shedlock, K. M., J. Baranowski, W. Xiao, and X. L. Hu, 1987: The Tangshan aftershock sequence. *J. Geophys. Res.*, **92**, 2791-2803, doi: 10.1029/JB092iB03p02791. [Link]

Sholupov, S., S. Pogarev, V. Ryzhov, N. Mashyanov, and A. Stroganov, 2004: Zeeman atomic absorption spectrometer RA-915+ for direct determination of mercury in air and complex matrix samples. *Fuel Process. Technol.*, **85**, 473-485, doi: 10.1016/j.fuproc.2003.11.003. [Link]

Sinclair, A. J., 1991: A fundamental approach to threshold estimation in exploration geochemistry: Probability plots revisited. *J. Geochem. Explor.*, **41**, 1-22, doi: 10.1016/0375-6742(91)90071-2. [Link]

Song, X., and B. V. Heyst, 2005: Volatilization of mercury from soils in response to simulated precipitation. *Atmos. Environ.*, **39**, 7494-7505, doi: 10.1016/j.atmosenv.2005.07.064. [Link]

Utkin, V. I. and A. K. Yurkov, 2010: Radon as a tracer of tectonic movements. *Russ. Geol. Geophys.*, **51**, 220-227, doi: 10.1016/j.rgg.2009.12.022. [Link]

Wakita, H., Y. Nakamura, I. Kita, N. Fujii, and K. Notsu, 1980: Hydrogen release: New indicator of fault activity. *Science*, **210**, 188-190, doi: 10.1126/science.210.4466.188. [Link]

Walia, V., H. S. Virk, and B. S. Bajwa, 2006: Radon precursory signals for some earthquakes of magnitude > 5 occurred in N-W Himalaya: An overview. *Pure Appl. Geophys.*, **163**, 711-721, doi: 10.1007/s00024-006-0044-z. [Link]

Walia, V., S. J. Lin, C. C. Fu, T. F. Yang, W. L. Hong, K. L. Wen, and C. H. Chen, 2010: Soil-gas monitoring: A tool for fault delineation studies along Hsinhua Fault (Tainan), Southern Taiwan. *Appl. Geochem.*, **25**, 602-607, doi: 10.1016/j.apgeochem.2010.01.017. [Link]

Wang, G., C. Liu, J. Wang, W. Liu, and P. Zhang, 2006: The use of soil mercury and radon gas surveys to assist the detection of concealed faults in Fuzhou City, China. *Environ. Geol.*, **51**, 83-90, doi: 10.1007/s00254-006-0306-1. [Link]

Washington, J. W. and A. W. Rose, 1992: Temporal variability of radon concentration in the interstitial gas of soils in Pennsylvania. *J. Geophys. Res.*, **97**, 9145-9159, doi: 10.1029/92JB00479. [Link]

Wiersberg, T. and J. Erzinger, 2008: Origin and spatial distribution of gas at seismogenic depths of the San Andreas Fault from drill-mud gas analysis. *Appl. Geochem.*, **23**, 1675-1690, doi: 10.1016/j.apgeochem.2008.01.012. [Link]

Woodruff, L. G., W. F. Cannon, D. D. Eberl, D. B. Smith, J. E. Kilburn, J. D. Horton, R. G. Garrett, and R. A. Klassen, 2009: Continental-scale patterns in soil geochemistry and mineralogy: Results from two transects across the United States and Canada. *Appl. Geochem.*, **24**, 1369-1381, doi: 10.1016/j.apgeochem.2009.04.009. [Link]

Yang, T. F., C. Y. Chou, C. H. Chen, L. L. Chyi, and J. H. Jiang, 2003: Exhalation of radon and its carrier gases in SW Taiwan. *Radiat. Meas.*, **36**, 425-429, doi: 10.1016/S1350-4487(03)00164-1. [Link]

Yang, T. F., C. C. Fu, V. Walia, C. H. Chen, L. L. Chyi, T. K. Liu, S. R. Song, M. Lee, C. W. Lin, and C. C. Lin, 2006: Seismo-geochemical variations in SW Taiwan: multi-parameter automatic gas monitoring results. *Pure Appl. Geophys.*, **163**, 693-709, doi: 10.1007/s00024-006-0040-3. [Link]

Zhou, X. C., J. G. Du, C. Y. Wang, Z. Q. Cao, L. Yi, and L. Liu, 2007 : Geochemical characteristics of radon and mercury in soil gas in Lhasa, Tibet, China. *Environ. Sci.*, **28**, 659-663. (in Chinese)